European Conference on Computational Fluid Dynamics
ECCOMAS CFD 2006
P. Wesseling, E. Oñate and J. Périaux (Eds)

CONVERGENCE ACCELERATION FOR THE THREE DIMENSIONAL COMPRESSIBLE NAVIER-STOKES EQUATIONS

E. Turkel[*], **V.N. Vatsa**[**], **R.C. Swanson** [†] **and C.-C. Rossow**[††]

[*] Tel-Aviv University, Dept. Mathematics, Israel
e-mail: turkel@post.tau.ac.il
[**] NASA Langley Research Center, Hampton,VA
e-mail: v.n.vatsa@larc.nasa.gov
[†] NASA Langley Research Center, Hampton,VA
e-mail: r.c.swanson.jr@larc.nasa.gov
[††] DLR, Braunschweig, Germany
e-mail: cord.rossow@dlr.de

Key words: Navier-Stokes, CFD, preconditioning, acceleration

Abstract. *We consider a multistage algorithm to advance in pseudo-time to find a steady state solution for the compressible Navier-Stokes equations. The rate of convergence to the steady state is improved by using an implicit preconditioner to approximate the numerical scheme. This properly addresses the stiffness in the discrete equations associated with highly stretched meshes. Hence, the implicit operator allows large time steps i.e. CFL numbers of the order of 1000. The proposed method is applied to three dimensional cases of viscous, turbulent flow around a wing, achieving dramatically improved convergence rates.*

1 INTRODUCTION

One of the most widespread relaxation methods is the class of schemes devised by Jameson, Schmidt and Turkel with extensions [2–4]. In this approach an explicit Runge-Kutta time integration scheme is augmented with implicit residual smoothing in combination with multigrid. This represents a well balanced compromise of simplicity in the basic explicit scheme and implicit consideration of the cell aspect ratio. Schemes based on this strategy have proven to be well suited for inviscid flow problems, and they allow for the successful solution of the Navier-Stokes equations. For viscous, turbulent flows, convergence rates deteriorate from rates in the order of 0.9-0.95, typically observed for inviscid flow, to 0.98-0.99.

One of the most promising general solution strategies is multigrid, which was originally developed to solve elliptic equations. Its extension to the Euler equations is still quite efficient. However, in contrast to the Euler equations, the solution of the Navier-Stokes equations still poses a formidable challenge. The main difficulty in computing viscous flow is that highly stretched meshes are required to economically resolve the steep gradients in the boundary layers, resulting in very high cell aspect ratios. These large cell aspect ratios lead to a severe

stiffness in the discrete system of equations, significantly reducing the efficiency of existing numerical algorithms. When using multigrid, the main ingredient is an appropriate relaxation method to smooth high frequency errors on the current mesh level. Explicit schemes have a low operation count per iteration and low storage requirements, but they have only limited stability imposed by the CFL condition. For explicit schemes with standard multigrid the convergence rate severely deteriorates on meshes with high aspect ratio cells. In contrast, implicit schemes theoretically offer unconditional stability, but they are computationally more expensive and incur a heavy memory overhead due to the storage of the flux Jacobian matrices. Therefore, in practice, approximate factorization such as ADI or LU is employed. The factorization error however prohibits the use of large time steps and thus limits the potential for fast convergence.

Rossow [9, 10] developed an efficient preconditioning that uses a first order upwind approximation to the equations. Using an economic evaluation of the flux Jacobians on the cell faces, a fully implicit operator is constructed to replace the implicit residual smoothing in the framework of the Runge-Kutta time stepping scheme. The approximate inverse of the implicit operator is obtained by performing several sweeps of symmetric Gauss-Seidel (GS). The symmetric Gauss-Seidel is applied as a sequence of forward and backward sweeps in each coordinate direction. Thus each symmetric sweep consists of two simple sweeps. In this paper we extend the implicit upwind preconditioner to three dimensions.

2 BASIC SCHEME

Consider the fluid equations in general coordinates ξ, η, ζ. We express the equations as

$$J^{-1}\frac{\partial W}{\partial t} = -\left\{\frac{\partial F}{\partial \xi} + \frac{\partial G}{\partial \eta} + \frac{\partial H}{\partial \zeta}\right\} = Res \tag{1}$$

J^{-1} is also the volume of a cell. This can also be expressed in quasi linear form as

$$J^{-1}\frac{\partial W}{\partial t} + A\frac{\partial W}{\partial \xi} + B\frac{\partial W}{\partial \eta} + C\frac{\partial W}{\partial \zeta} = 0$$

where A and B are the flux Jacobian matrices defined by $A = \frac{\partial F}{\partial W}$, $B = \frac{\partial G}{\partial W}$. and $C = \frac{\partial H}{\partial W}$.

We shall discretize (1) by considering the space and time portions separately. The unknown variables W are located at the center of a cell. We discretize the fluxes by a central difference, i.e. F and G are located at the faces of the cell and are evaluated by an arithmetic average from the neighboring cell centers. This central difference allows high frequency waves to persist. Furthermore, it is nonlinearly unstable in the presence of shocks. Hence, we add a matrix viscosity [12] to stabilize the scheme. The dissipation terms are a blending of second and fourth differences.

$$AD = \left(D_\xi^2 + D_\eta^2 + D_\zeta^2 - D_\xi^4 - D_\eta^4 - D_\zeta^4\right) W, \tag{2}$$

where

$$D_\xi^2 W = \nabla_\xi \left[\left(|A|_{i+\frac{1}{2},j,k}\epsilon^2_{i+\frac{1}{2},j,k}\right)\Delta_\xi\right] W_{i,j,k} \tag{3}$$

$$D_\xi^4 W = \nabla_\xi \left[\left(|A|_{i+\frac{1}{2},j,k} \epsilon^{(4)}_{i+\frac{1}{2},j,k} \right) \Delta_\xi \nabla_\xi \Delta_\xi \right] W_{i,j,k} \tag{4}$$

and Δ_ξ, ∇_ξ are the standard forward and backward difference operators respectively associated with the ξ direction. The coefficients $\epsilon^{(2)}$ and $\epsilon^{(4)}$ are adapted to the flow as follows:

$$\begin{aligned}
\epsilon^{(2)}_{i+\frac{1}{2},j,k} &= \kappa^{(2)} \max(\nu_{i-1,j,k}, \nu_{i,j}, \nu_{i+1,j,k}, \nu_{i+2,j,k}) \\
\nu_{i,j,k} &= \left| \frac{p_{i+1,j,k} - 2p_{i,j,k} + p_{i-1,j,k}}{p_{i+1,j,k} + 2p_{i,j,k} + p_{i-1,j,k}} \right| \\
\epsilon^{(4)}_{i+\frac{1}{2},j,k} &= \max \left[0, \left(\kappa^{(4)} - \epsilon^{(2)}_{i+\frac{1}{2},j,k} \right) \right]
\end{aligned}$$

where p is the pressure, and the quantities $\kappa^{(2)}$ and $\kappa^{(4)}$ are constants to be specified. The operators in (2) for the η and ζ directions are defined in a similar manner.

The second-difference dissipation term is nonlinear. Its purpose is to introduce an entropy-like condition and to suppress oscillations in the neighborhood of shocks. This term is small in the smooth portion of the flow field. The fourth-difference dissipation term is basically linear and is included to damp high-frequency modes and allow the scheme to approach a steady state. Only this term affects the linear stability of the scheme. Near shocks it is reduced to zero.

To advance the scheme in time we use a multistage scheme with n stages. A typical stage of the Runge-Kutta approximation to (1) is

$$W^k - W^0 = \alpha_k \frac{\Delta t}{\text{Vol}} \left[D_\xi F^{(k-1)} + D_\eta G^{(k-1)} + D_\zeta H^{(k-1)} - AD \right] = Res^{k-1} \tag{5}$$

where D_ξ and D_η are spatial differencing operators, and AD represents the artificial dissipation terms. This scheme is only first order in time. However, as we approach the steady state the accuracy in time is meaningless. To increase the efficiency of the scheme and also increase the stability region of the method it is useful to not recalculate AD at each stage but rather only some stages and use averages of these values within (5).

To accelerate the convergence to a steady state we consider a multigrid method [4] with the Runge-Kutta method as the smoother. As an additional acceleration technique we implicitly smooth [4] the residuals Res^{k-1}. Thus, we replace Res^{k-1} in (5) by $\widehat{Res}^{k-1}$ where

$$\left(I - \gamma (D_\xi^2 + D_\eta^2 + D_\zeta^2) \right) \widehat{Res}^{k-1} = Res^{k-1}$$

where γ depends on the ratio of the new CFL number to the original CFL number. Since it is difficult to directly invert the three dimensional operator we replace this by a dimensional split [3],

$$\left(I - \gamma_\xi D_\xi^2 \right) \left(I - \gamma_\eta D_\eta^2 \right) \left(I - \gamma_\zeta D_\zeta^2 \right) \widehat{Res}^{k-1} = Res^{k-1} \tag{6}$$

The various γ_i can be made functions of the aspect ratios in each direction [6].

Rossow [9, 10] suggested replacing this implicit residual smoothing by a more appropriate preconditioning based on a first order upwind scheme. Thus we replace (6) by

$$\left(I + \frac{\Delta t}{\text{vol}} \sum_{\text{all faces}} A^+ S \right) \widehat{Res}^{k-1} = Res^{k-1} - \sum_{\text{all faces}} A^- S \widehat{Res}^{k-1}_{NB} \tag{7}$$

where S is the area of a face, and NB refers to all direct neighbors of the cell being considered which depends on the direction within the Gauss-Seidel sweep. This is now an implicit method to find the smoothed residual. To approximately invert the implicit operator of (7) we use several (typically 2-3) symmetric point Gauss-Seidel sweeps. These are started with an initial guess of zero. This still requires the inversion of a local 5×5 matrix at every grid point in each sweep. To increase efficiency, the system is converted to primitive variables, (ρ, p, u, v, w), which reduces the number of operations in inverting the local matrix.

3 ABSOLUTE VALUE MATRIX

We now consider, in more detail, the structure and properties of the matrices A^+, A^- and $|A| = A^+ - A^-$. In addition to the usual speed of sound c, define a modified speed of sound $\widehat{c}$. We shall later distinguish between them. Let (S_x, S_y, S_x) denote the three components of the surface area normal to the x direction. There are similar matrices $|B|$ and $|C|$ using the surface area normal to the y and z directions, respectively. Define $|S| = \sqrt{S_x^2 + S_y^2 + S_z^2}$. The contravariant velocity is given by $U = uS_x + vS_y + wS_z$ and the directional Mach number is $M = \frac{U}{c|S|}$. To simplify the matrix we predefine some notation. Let $T = (1 - |M|)|S|\widehat{c} + \frac{\mu}{3}$, $R = \frac{|S|(1-|M|)}{\widehat{c}}$ and $U^+ = U + |U|$, $U^- = U - |U|$. U and M are prevented from getting too small by factors that include some constants and aspect ratios.

To derive the absolute value of the Jacobian matrices it is easier to work with the entropy variables $(\frac{dp}{\rho c}, du, dv, dw, dS)$ with $dS = dp - c^2 d\rho$. Note, that in addition to changing from the density ρ to the entropy S we have also changed the order of the variables. We denote A_S as the Jacobian matrix with respect to the entropy variables. We use the following combination of eigenvalues

- $Q_+ = \frac{|U+c|S||+|U-c|S||}{2}$
- $Q_- = \frac{|U+c|S||-|U-c|S||}{2}$
- $Q_0 = Q_+ - |U|$

For subsonic flow this reduces to

- $Q_+ = c|S|$
- $Q_- = |U|$
- $Q_0 = c|S| - |U| = c|S|(1 - |M|) = T$

We calculate the absolute value of a matrix by diagonalizng, taking the absolute values and transforming back. Assuming $\widehat{c}=c$ then $Q_0=|S|T$ and $|U|+Rc^2=|U|+|S|(1-\frac{U}{c|S|})c=c|S|$. So in entropy variables we have for the inviscid terms

$$A_S=\begin{pmatrix} U & S_xc & S_yc & S_zc & 0\\ S_xc & U & 0 & 0 & 0\\ S_yc & 0 & U & 0 & 0\\ S_zc & 0 & 0 & U & 0\\ 0 & 0 & 0 & 0 & U \end{pmatrix}$$

We define the normalized surface areas by $\widehat{S}_x=\frac{S}{|S|}$ etc. Then

$$\begin{aligned} |A_S| &= \begin{pmatrix} Q_+ & \widehat{S}_xQ_- & \widehat{S}_yQ_- & \widehat{S}_zQ_- & 0\\ \widehat{S}_xQ_- & |U|+\widehat{S}_x^2Q_0 & \widehat{S}_x\widehat{S}_yQ_0 & \widehat{S}_x\widehat{S}_zQ_0 & 0\\ \widehat{S}_yQ_- & \widehat{S}_x\widehat{S}_yQ_0 & |U|+\widehat{S}_y^2Q_0 & \widehat{S}_y\widehat{S}_zQ_0 & 0\\ \widehat{S}_zQ_- & \widehat{S}_x\widehat{S}_zQ_0 & \widehat{S}_y\widehat{S}_zQ_0 & |U|+\widehat{S}_z^2Q_0 & 0\\ 0 & 0 & 0 & 0 & |U| \end{pmatrix}\\ &\overset{subsonic}{=} \begin{pmatrix} c|S| & \widehat{S}_xQ_- & \widehat{S}_yQ_- & \widehat{S}_zQ_- & 0\\ \widehat{S}_xQ_- & |U|+\widehat{S}_x^2T & \widehat{S}_x\widehat{S}_yT & \widehat{S}_x\widehat{S}_zT & 0\\ \widehat{S}_yQ_- & \widehat{S}_x\widehat{S}_yT & |U|+\widehat{S}_y^2T & \widehat{S}_y\widehat{S}_zT & 0\\ \widehat{S}_zQ_- & \widehat{S}_x\widehat{S}_zT & \widehat{S}_y\widehat{S}_zT & |U|+\widehat{S}_z^2T & 0\\ 0 & 0 & 0 & 0 & |U| \end{pmatrix}\\ &= \begin{pmatrix} |U|+Rc^2 & S_x|M|c & S_y|M|c & S_z|M|c & 0\\ S_x|M|c & |U|+\widehat{S}_x^2T & \widehat{S}_x\widehat{S}_yT & \widehat{S}_x\widehat{S}_zT & 0\\ S_y|M|c & \widehat{S}_x\widehat{S}_yT & |U|+\widehat{S}_y^2T & \widehat{S}_y\widehat{S}_zT & 0\\ S_z|M|c & \widehat{S}_x\widehat{S}_zT & \widehat{S}_y\widehat{S}_zT & |U|+\widehat{S}_z^2T & 0\\ 0 & 0 & 0 & 0 & |U| \end{pmatrix} \end{aligned}$$

(see e.g. [5, 17, 18]), $A_S^+=\frac{A_s+|A_s|}{2}$, $|U|+Rc^2\to\frac{c^2}{\widehat{c}}|S|+|U|(1-\frac{c}{\widehat{c}})$.

We next consider the accuracy for low Mach number flows. From [14] a necessary condition that the solution of the compressible equations converges to the solution of the incompressible equations, as $M_\infty\to 0$, is

$$|A_S|\sim \begin{pmatrix} O\left(\frac{1}{M_\infty^2}\right) & O\left(\frac{1}{M_\infty}\right) & O\left(\frac{1}{M_\infty}\right) & O\left(\frac{1}{M_\infty}\right) & 0\\ O\left(\frac{1}{M_\infty}\right) & O(1) & & & 0\\ O\left(\frac{1}{M_\infty}\right) & & O(1) & & 0\\ O\left(\frac{1}{M_\infty}\right) & & & O(1) & 0\\ 0 & 0 & 0 & 0 & O(1) \end{pmatrix} \qquad \text{as } M_\infty\to 0$$

with all the non-given terms also $O(1)$. We see that this is true if and only if we precondition the speed of sound so that R and T are $O(1)$. Hence, $\widehat{c} = O(1)$ while $c = O\left(\frac{1}{M_\infty}\right)$. One way to accomplish this is to choose

$$\begin{aligned} M_{ref}^2 &= \min\left\{\max(\frac{q^2}{c^2}, M_\infty^2)\right\} \\ \alpha &= \frac{1 - M_{ref}^2}{2} \\ \widehat{c}^2 &= (\alpha q)^2 + q_{ref}^2 \end{aligned} \tag{8}$$

see, for example, [8,13]. For transonic flow $\widehat{c}$ is close to c while for low speed flow $\widehat{c}$ behaves like the convective speed, q. In the computations we have not used any low speed preconditioning [13, 15, 16] or the modified $\widehat{c}$ for the case with $M_\infty = 0.30$ since the artificial viscosity is not modified to handle this case.

Returning to primitive variables (ρ, p, u, v, w), we first consider the inviscid contribution. Initially we use $A_S^+ = \frac{A_S + |A_S|}{2}$, and then convert from entropy variables to primitive variables. Let $Y = 1 + \frac{Q_-}{c|S|}$. This gives

$$\begin{aligned} A^+ =& \frac{1}{2}\begin{pmatrix} U^+ & \frac{Q_+ - |U|}{c^2} & \rho S_x Y & \rho S_y Y & \rho S_z Y \\ 0 & Q_+ + U^+ & S_x \rho c^2 Y & S_y \rho c^2 Y & S_z \rho c^2 Y \\ 0 & \frac{S_x}{\rho} Y & U^+ + \widehat{S}_x^2 Q_0 & \widehat{S}_x \widehat{S}_y Q_0 & \widehat{S}_x \widehat{S}_z Q_0 \\ 0 & \frac{S_y}{\rho} Y & \widehat{S}_x \widehat{S}_y Q_0 & U^+ + \widehat{S}_y^2 Q_0 & \widehat{S}_y \widehat{S}_z Q_0 \\ 0 & \frac{S_z}{\rho} Y & \widehat{S}_x \widehat{S}_z Q_0 & \widehat{S}_y \widehat{S}_z Q_0 & U^+ + \widehat{S}_z^2 Q_0 \end{pmatrix} \\ \overset{subsonic}{=} & \frac{1}{2}\begin{pmatrix} U^+ & R & S_x \rho (1+M) & S_y \rho (1+M) & S_z \rho (1+M) \\ 0 & U^+ + Rc^2 & S_x \rho c^2 (1+M) & S_y \rho c^2 (1+M) & S_z \rho c^2 (1+M) \\ 0 & S_x \frac{(1+M)}{\rho} & U^+ + \widehat{S}_x^2 T & \widehat{S}_x \widehat{S}_y T & \widehat{S}_x \widehat{S}_z T \\ 0 & S_y \frac{(1+M)}{\rho} & \widehat{S}_x \widehat{S}_y T & U^+ + \widehat{S}_y^2 T & \widehat{S}_y \widehat{S}_z T \\ 0 & S_z \frac{(1+M)}{\rho} & \widehat{S}_x \widehat{S}_z T & \widehat{S}_y \widehat{S}_z T & U^+ + \widehat{S}_z^2 T \end{pmatrix} \end{aligned}$$

To this we add a viscous contribution. For the examples in this paper we only add these in the η direction. This is given by

$$B = \frac{\alpha}{\rho Vol}\begin{pmatrix} 0 & 0 & 0 & 0 & 0 \\ B_{21} & B_{22} & 0 & 0 & 0 \\ 0 & 0 & B_{33} & B_{34} & B_{35} \\ 0 & 0 & B_{43} & B_{44} & B_{45} \\ 0 & 0 & B_{53} & B_{54} & B_{55} \end{pmatrix}$$

Define $\alpha = \frac{\sqrt{\gamma} M_\infty}{Re}$. This contribution arises from the nondimensionalization in the code. Then

we have

$$
\begin{aligned}
B_{21} &= -\gamma \frac{\mu}{Pr} \frac{p}{\rho} |\nabla \eta|^2 \\
B_{22} &= \gamma \frac{\mu}{Pr} |\nabla \eta|^2 \\
B_{33} &= (\lambda + \mu) \eta_x^2 + \mu |\nabla \eta|^2 \\
B_{44} &= (\lambda + \mu) \eta_y^2 + \mu |\nabla \eta|^2 \\
B_{55} &= (\lambda + \mu) \eta_z^2 + \mu |\nabla \eta|^2 \\
B_{43} = B_{34} &= (\lambda + \mu) \eta_x \eta_y \\
B_{53} = B_{35} &= (\lambda + \mu) \eta_x \eta_z \\
B_{54} = B_{45} &= (\lambda + \mu) \eta_y \eta_z
\end{aligned}
$$

We choose $\lambda = -\frac{2}{3}\mu$. The term B_{21} destroys the zero structure of the first column (below the diagonal) of the matrix. Hence, for convenience it is neglected.

4 RESULTS

We assess the results for the computation of viscous, turbulent airfoil flow about an ONERA M6 wing, with a $192 \times 48 \times 32$ C-O mesh at an angle of attack $\alpha = 3.06^\circ$ and a Reynolds number of $Re = 21.158$ million using a Baldwin Lomax turbulence model. All schemes are run with a local time step, matrix viscosity, multigrid and a five stage Runge-Kutta smoother. For the standard scheme we use Runge-Kutta coefficients $\alpha_k = .25, .1667, .375, .5, 1.0$. We update the artificial viscosity on the first, third and fifth stages. These are combined, on the odd stages, with the previous artificial viscosity using weights of $1, .56, .44$. For the upwind preconditioning we treat the scheme as an upwind scheme even though the major discretization is a central difference with a matrix viscosity. This is feasible because a matrix viscosity makes the scheme similar to an upwind scheme. Computationally, we have found that when using a scalar viscosity on the finest mesh that the scheme no longer converges. Nevertheless, we do use a scalar viscosity on all the coarser meshes. However, one must decrease the coefficient of the scalar artificial viscosity on the coarse grids by a factor of about 3-5 compared with the standard scheme. For the new upwind preconditioner we choose Runge Kutta coefficients $.0695, .1602, .2898, .506, 1.0$. The artificial viscosity is now evaluated at every stage which also increases the cost of the new scheme. The residual smoothing of the original scheme allows a CFL of 6.5. With the new upwind preconditioning we use a CFL of 1000.

We now compare the performance of these two schemes for a range of Mach numbers. The first case we consider is an inflow Mach number $M_\infty = 0.84$. For this transonic case the change to $\widehat{c}$ has a minor impact. We first present a comparison of the convergence rate of the residual and lift. Both codes were begun on the finest mesh, with a constant flow initialization, without obtaining a better initial guess from a sequence of coarser meshes (FMG). We stress that both runs were identical except for the calls to either residual smoothing or else to the new implicit upwind preconditioner. As noted above there are differences in the input parameters as to the

CFL number, Runge-Kutta coefficients, level of artificial viscosity on the coarse grids and times where the artificial viscosity is evaluated.

None of these differences should effect the final converged solution. To demonstrate the accuracy of the solution we compare, for $M_\infty = 0.84$, in figures 1 through 4, the computed pressure distributions with experimental data [11] at four spanwise locations.

The improved convergence rate demonstrates the potential of the present approach. On a DEC single processor workstation the standard code required about 320 minutes for 1200 time cycles while the new algorithm required about 200 minutes for 200 time cycles. Hence, the upwind preconditioner code is about four times slower per iteration than the implicit residual smoothing code even though we use three symmetric Gauss-Seidel sweeps to invert the preconditioner. We also did runs with only two symmetric point Gauss-Seidel sweeps using four permutations of sweep directions (backward in all directions, forward only in j, backward only in j, and forward in all directions). This required about 160 minutes for the same 200 MG iterations. In summary, to reduce the residual by six orders of magnitude the standard scheme required 1027 iterations and 273 seconds. The new implicit method with three symmetric GS sweeps required 48 iterations and 48 seconds which gives an efficiency factor of 5.7. When using two symmetric GS sweeps, 51 iterations were required which took 40.8 seconds and so is 6.7 times faster than the standard scheme. We see this graphically in figure 5. For the convergence of the lift, figure 6, and drag, figure 7, it is difficult to distinguish between the cases with two or three symmetric GS sweeps. The plots for lift and drag only display the first 200 iterations so that the difference between the two convergence rates is clearer. So we get similar increases in efficiency based on converging the lift and drag rather than reducing the residual.

We next consider, in figures 8-10, the same parameters, with three symmetric GS sweeps, but with $M_\infty = 0.95$. In figures 11-13 we present the results for the supersonic case, with $M_\infty = 1.10$. For these cases we get a similar improvement but the reduction in the residual is a little less. For $M_\infty = 1.20$ (not shown) we get a more substantial slowdown in convergence. We note, that the grid is not appropriate for supersonic flow. Finally, in figures 14-16 we consider the case with $M_\infty = 0.30$. To use the low speed modifications to the speed of sound c one must modify not only the acceleration techniques but also the artificial viscosity. Since this was not done we do not employ the change of $\widehat{c}$ for low speed and and do not use any low speed preconditioning [13–17, 19]. Now, the residual reduction, with the new upwind preconditioner, is even slower but still much more efficient than the code with residual smoothing. The lift and drag are now displayed for a total of 600 iterations to see the difference in convergence rates. In table 1 we present the average convergence rate of the residual for each case at the end of the computation.

Mach	type	avg conv rate
0.30	standard	.989
0.30	implicit	.922
0.84	standard	.987
0.84	implicit	.879
0.84	implic-4	.883
0.95	standard	.987
0.95	implicit	.887
1.05	standard	.987
1.05	implicit	.886
1.10	implicit	.888
1.20	standard	.993
1.20	implicit	.941

Table 1: Comparison of inviscid lift and drag with/without preconditioning

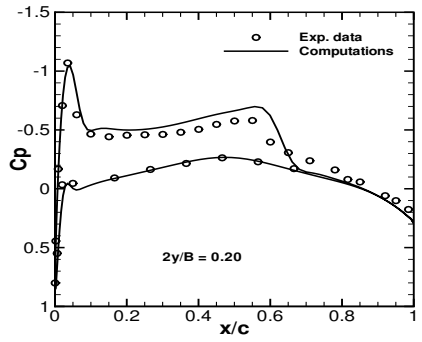

Figure 1: C_p at station 0.20

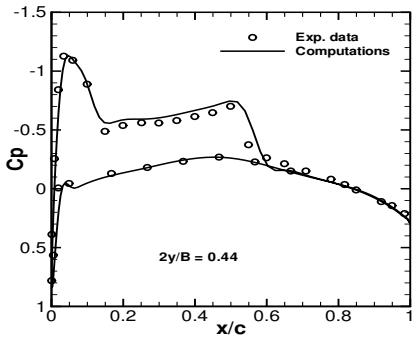

Figure 2: C_p at station 0.44

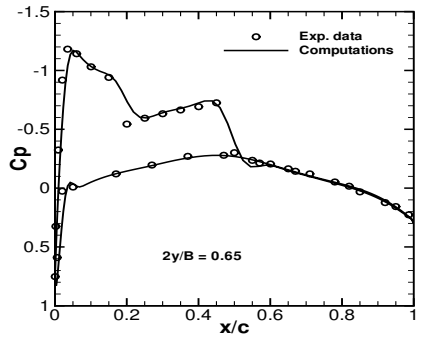

Figure 3: C_p at station 0.65

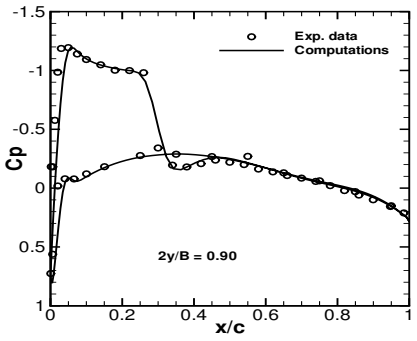

Figure 4: C_p at station 0.90

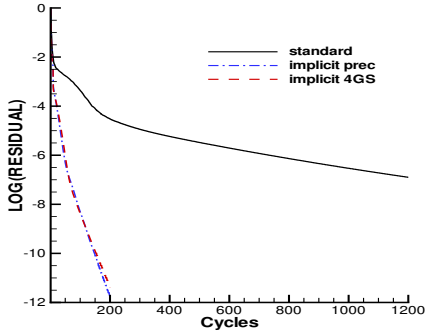

Figure 5: Residual Convergence, $M_\infty = 0.84$

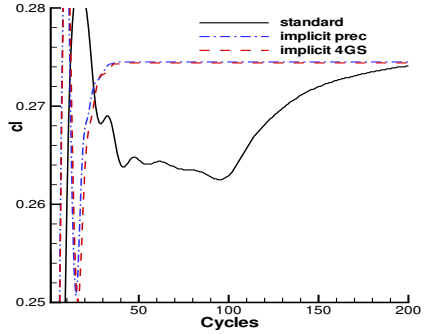

Figure 6: Lift convergence for $M_\infty = 0.84$

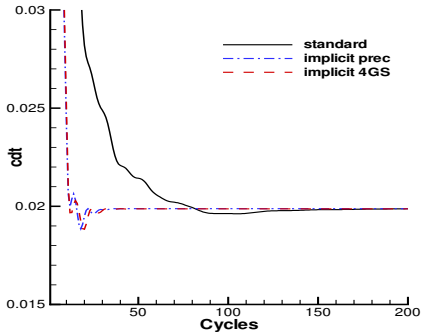

Figure 7: Drag Convergence for $M_\infty = 0.84$

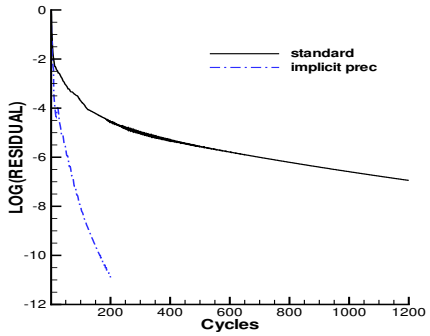

Figure 8: Residual convergence, $M_\infty = 0.95$

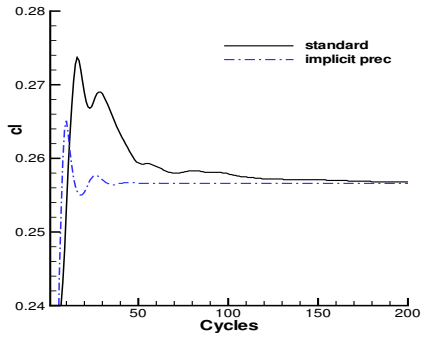

Figure 9: Lift Convergence for $M_\infty = 0.95$

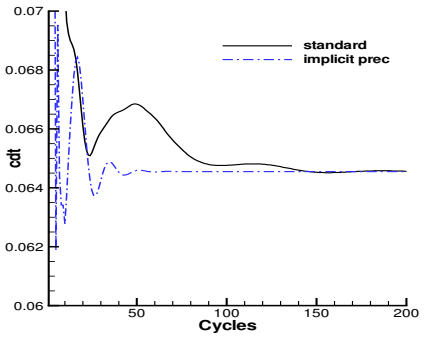

Figure 10: Drag convergence for $M_\infty = 0.95$

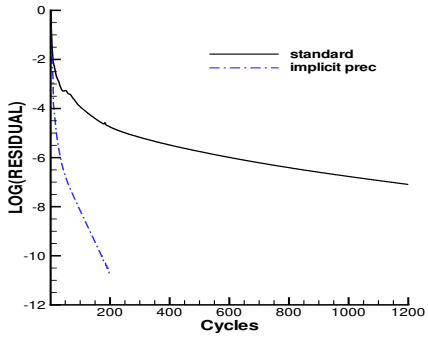

Figure 11: Residual Convergence $M_\infty = 1.10$

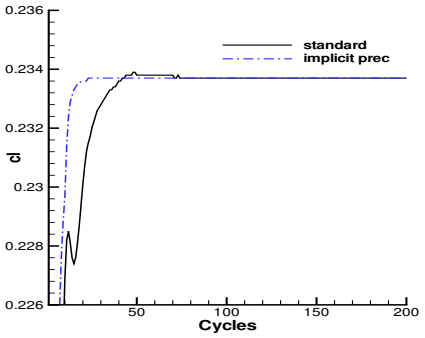

Figure 12: Lift convergence for $M_\infty = 1.10$

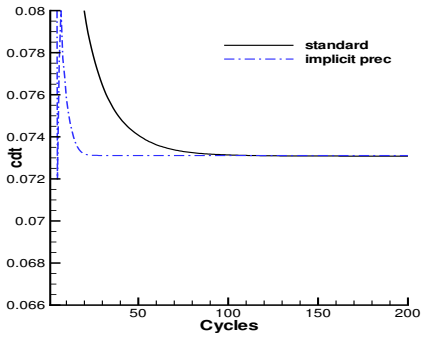

Figure 13: Drag Convergence for $M_\infty = 1.10$

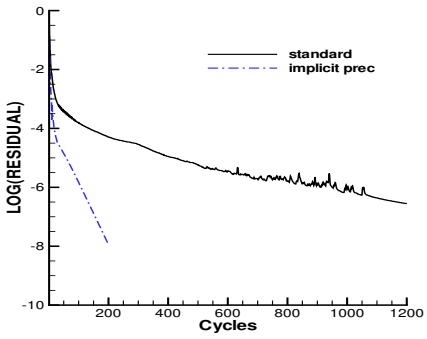

Figure 14: Residual Convergence $M_\infty = 0.30$

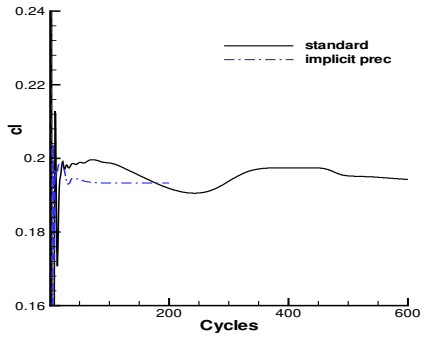

Figure 15: Lift convergence for $M_\infty = 0.30$

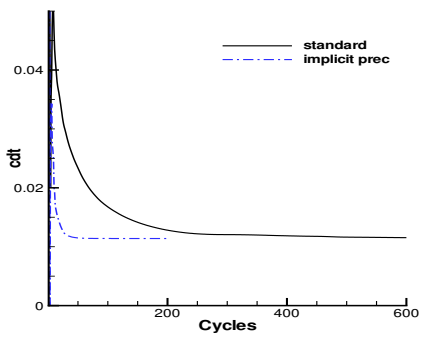

Figure 16: Drag Convergence for $M_\infty = 0.30$

5 CONCLUSIONS

We consider a central difference approximation to the compressible Navier-Stokes equations. For stability this is supplemented by a matrix viscosity using a combination of second and fourth differences. To advance in time we use a multistage scheme coupled with multigrid. The usual residual smoothing is replaced by a first order upwind scheme. This is inverted by point Gauss-Seidel iterations.

We consider an application to three dimensional turbulent flow over an ONERA M6 wing for a range of Mach numbers. It is demonstrated that the new preconditioner leads to a dramatic increase in efficiency. We also consider modifications for low speed flow.

REFERENCES

[1] D.A. Caughey and A. Jameson. Fast Preconditioned Multigrid Solution of the Euler and Navier-Stokes Equations for Steady, Compressible Flows, *AIAA-Paper*, **2002–0963** (2002).

[2] A. Jameson, W. Schmidt and E. Turkel. Numerical Solutions of the Euler Equations by Finite Volume Methods Using Runge-Kutta Time-Stepping Schemes, *AIAA-Paper*, **81–1259** (1981).

[3] A. Jameson. The Evolution of Computational Methods in Aerodynamics, *J. Appl. Mech.*, **50** 1052–1070, (1983).

[4] A. Jameson. Multigrid Algorithms for Compressible Flow Calculations, *Second European Conference on Multigrid Methods*, Cologne, 1985, ed. W. Hackbusch and U. Trottenberg, Lecture Notes in Mathematics, Vol. 1228, Springer Verlag, Berlin, (1986).

[5] A. Jameson and D.A. Caughey. How Many Steps are Required to Solve the Euler Equations of Steady, Compressible Flow: In Search of a Fast Solution Algorithm, *AIAA-Paper*, **2001–2673** (2001).

[6] L. Martinelli and A. Jameson. Validation of a Multigrid Method for the Reynolds Averaged Equations, *AIAA-Paper*, **88–0414** (1988).

[7] C.-C. Rossow. A Flux Splitting Scheme for Compressible and Incompressible Flows, *J. Comp. Phys.*, **164** 104–122, (2000).

[8] C.-C. Rossow. Extension of a Compressible Code Toward the Incompressible Limit, *AIAA J.*, **41** 2379–2386, (2003).

[9] C.-C. Rossow. Convergence Acceleration for Solving the Compressible Navier-Stokes Equations, *AIAA J.*, **44** 345–352, (2006).

[10] C.-C. Rossow, Efficient Computation of Compressible and Incompressible Flows, to appear in *J. Comp. Phys.*

[11] V. Schmitt and F. Charpin. Pressure Distributions on the ONERA-M6-Wing at transonic Mach numbers, *AGARD-AR-138,* Chap B-1, May (1979).

[12] R.C. Swanson and E. Turkel. On Central Difference and Upwind Schemes, *J. Comp. Phys.*, **101** 292–306, (1992).

[13] E. Turkel. Preconditioned Methods for Solving the Incompressible and Low Speed Compressible Equations, *J. Comp. Phys.*, **72** 277–298, (1987).

[14] E. Turkel, A. Fiterman and B. van Leer. Preconditioning and the Limit of the Compressible to the Incompressible Flow Equations for Finite Difference Schemes, *Frontiers of Computational Fluid Dynamics 1994*, 215–234. D.A. Caughey and M.M. Hafez editors, John Wiley and Sons, (1994).

[15] E. Turkel. Review of Preconditioning Methods for Fluid Dynamics, *Appl. Numer. Math.*,**12** 257–284, (1993).

[16] E. Turkel. Preconditioning Techniques in Computational Fluid Dynamics, *Annual Rev. Fluid Mech.* **31** 385–416, (1999).

[17] E. Turkel and V.N. Vatsa. Local Preconditioners for Steady State and Dual Time-Stepping, *Mathematical Modeling and Numerical Analysis, ESAIM: M2AN* **39**, 515–536, (2005).

[18] V.N. Vatsa and E. Turkel. Assessment of Local Preconditioners for Steady State and Time Dependent Flows, *AIAA-Paper*, **2004–2134** (2004).

[19] J.M. Weiss and W.A. Smith. Preconditioning Applied to Variable and Constant Density Flows, *AIAA J.*, **33** 2050–2057, (1995).